

# Beamline X29: a novel undulator source for X-ray crystallography

Wuxian Shi,<sup>a</sup> Howard Robinson,<sup>b</sup> Michael Sullivan,<sup>a</sup> Don Abel,<sup>a</sup>  
John Toomey,<sup>a</sup> Lonny E. Berman,<sup>c</sup> Don Lynch,<sup>c</sup> Gerd Rosenbaum,<sup>d</sup>  
George Rakowsky,<sup>c</sup> Larry Rock,<sup>e</sup> Bill Nolan,<sup>b</sup> Grace Shea-McCarthy,<sup>b</sup>  
Dieter Schneider,<sup>b</sup> Erik Johnson,<sup>c</sup> Robert M. Sweet<sup>b</sup> and Mark R. Chance<sup>a\*</sup>

<sup>a</sup>Center for Synchrotron Biosciences, Case Proteomics Center, Case Western Reserve University, 10900 Euclid Avenue, Cleveland, OH 44106, USA, <sup>b</sup>Protein Crystallography Research Resource, Biology Department, Brookhaven National Laboratory, Upton, NY 11973, USA, <sup>c</sup>National Synchrotron Light Source, Brookhaven National Laboratory, Upton, NY 11973, USA, <sup>d</sup>Department of Biochemistry, University of Georgia, Southeast Regional CAT at the APS, Argonne National Laboratory, Argonne, IL 60439, USA, and <sup>e</sup>LR DESIGN, Scottsdale, AZ, USA.  
E-mail: mark.chance@case.edu

A high-flux insertion device and beamline for macromolecular crystallography has been built at the National Synchrotron Light Source (NSLS) that employs a mini-gap undulator source developed by the NSLS. The mini-gap undulator at beamline X29 is a hybrid-magnet device of period 12.5 mm operating at proven gaps of 3.3–10 mm. The beamline provides hard X-rays for macromolecular crystallography experiments from the second and third harmonics over an energy range of 5–15 keV. The X-ray optics is designed to deliver intense and highly collimated X-rays. Horizontal focusing is achieved by a cryogenically cooled sagittally focusing double-crystal monochromator with ~4.1:1 demagnification. A vertical focusing mirror downstream of the monochromator is used for harmonic rejection and vertical focusing. The experimental station hosts an Area Detector Systems Quantum 315 CCD detector with 2.2 s readout time between exposures and Crystal Logic goniostat for crystal rotation and detector positioning. An auto-mounter crystal changer has been installed to facilitate the high-throughput data collection required by the major users, which includes structural genomics projects and the Macromolecular Crystallography Research Resource mail-in program. X29 is  $10^3$  times brighter than any existing bending-magnet beamline at NSLS with an actual flux of  $2.5 \times 10^{11}$  photons  $s^{-1}$  through a 0.12 mm square aperture at 11.271 keV.

## 1. Introduction

Both the brightness (intensity with fine collimation) and tunability of synchrotron sources contribute significantly to their value in structural biology experiments. The broad-band nature of synchrotron radiation sources allows for highly efficient structure determination by single- or multiple-wavelength anomalous dispersion (SAD or MAD) techniques. In many cases the high brightness of synchrotron X-ray beamlines provides a significant enhancement in the resolution of data collected from weakly diffracting crystals. Studies of macromolecular assemblies are often plagued by such weakly diffracting and small crystals. Even when focused bending-magnet sources are employed to examine such problems, data adequate to appreciate the reaction mechanism fully cannot

always be obtained. Insertion devices (IDs) are critical for solving these difficult crystallographic problems.

Numerous ID stations have been established in the USA and around the world in the last five years. There are eight ID beamlines currently available and two new ID beamlines in commissioning phases that are suitable for macromolecular crystallography studies at the Advanced Photon Source (APS), either partially or primarily open to the general user community (<http://biosync.rcsb.org/aps/aps.html>). At the Advanced Light Source, an excellent wiggler line has been in operation for some time. In addition, bright 'superbend' beamlines providing additional high flux and brightness have been built for crystallography (MacDowell *et al.*, 2004). At Stanford Synchrotron Radiation Laboratory (SSRL) all the ID stations have received upgrades to accommodate a ring

upgrade that will provide enhanced flux and brightness for the several crystallography beamlines as well as for other experiments. At Cornell High Energy Synchrotron Source, ID crystallography has a long history, and the wigglers there have undergone a program of continual improvement. These programs attest to the significant demand for experimental stations of this type, and indicate that the regional communities involved (especially the West Coast and Mid-West of USA) are quite well served by the existing plans.

At the NSLS, the X25 wiggler had been an invaluable source to the macromolecular crystallography community, especially those in the Mid-Atlantic region and New England. However, users at the NSLS are quite numerous, with approximately 900 active users having recently come to the facilities to perform macromolecular crystallography experiments; over 50% of the beam-time requests have listed the X25 station as their first choice. Even though nearly all of the available beam time is available to the outside community, only short intervals of beam time were available during each four-month scheduling period for those investigators who were awarded time. It was clear that a new ID source dedicated to crystallography would be extensively used, of great value to the users, and would help to solve difficult and interesting problems important to biology. Construction of such a device was warranted at the NSLS, both from the standpoint of internal demand figures and from the standpoint of national trends in ID availability and utilization.

At NSLS, the beamlines with designations X[4*n* + 1], where *n* = 0 to 7, are those in straight sections where multi-magnet devices like wigglers or undulators might be inserted. The only two remaining straight sections uncommitted to insertion devices were X9 and X29 (*n* = 2, 7). Radio frequency (RF) cavities that replenish the storage-ring energy in these locations occupied space that would be necessary for the insertion of one of these devices. X9 currently houses strong bending-magnet crystallography and EXAFS programs; moving them would be costly and time-consuming, although ultimately it will be desirable to do so. This leaves X29, which had no program or beamline in place, and thus was immediately available for use. To allow the placement of a mini-gap undulator in the X29 straight sections, the NSLS has designed new (and more powerful) RF cavities that could be placed further apart. The replacement of the RF cavities allowed the proposed new undulator to be inserted between them, thus recapturing the X29 straight section for high-impact scientific uses.

The third-generation synchrotron sources such as APS, the European Synchrotron Radiation Facility and SPring-8 represent the highest-energy rings (6–8 GeV) for synchrotron radiation in the world. The high ring energy provides hard X-rays from conventional undulators, and the brightness of these conventional undulator devices is extreme. For example, for the APS undulator-A design (at 100 mA at ~14 mm gap) the brilliance at the peak of the first harmonic (~7 keV, ~17 mm gap) is ~3 × 10<sup>19</sup> photons s<sup>-1</sup> (0.1% bandwidth)<sup>-1</sup> mrad<sup>-2</sup> mm<sup>-2</sup> (100 mA)<sup>-1</sup> (Dejus *et al.*, 2002).

Research has been carried out in directions intended to approach this performance with lower ring energy. A short-period mini-gap undulator (MGU) that produces high-brightness photon beams in the hard X-ray region installed in moderate-energy electron storage rings has been developed at NSLS and installed at X29. Compared with the conventional undulators at APS and other high-energy sources, the MGU at X29 is smaller, more cost-effective, and provides hard X-rays at lower ring energy (2.8 GeV). The success in implementing the MGU technology has greatly increased the performance of other synchrotron radiation rings like the Swiss Light Source. For other new rings, like DIAMOND in the UK, as well as for undeveloped straight sections at SSRL-SPEAR, MGUs have been highly competitive beamline options from the standpoint of both performance and cost. The successful development and implementation of the MGU at NSLS provides an example of world-wide dissemination of this technology to the 2–3 GeV rings.

## 2. Mini-gap undulator

In December 2003, the installation of the X29 MGU was completed. The X29 MGU occupies a narrow space between two new RF cavities in the NSLS X29 straight section. X29 is optimized for the needs of the structural biology program. For macromolecular crystallography the energy range of interest is approximately 7–15 keV. The radiated wavelength  $\lambda$  from an undulator is

$$\lambda = \frac{\lambda_u}{2n\gamma^2} (1 + K^2/2).$$

$\lambda_u$  is the undulator period, *n* is the harmonic number,  $\gamma$  is the electron beam energy in units of rest energy, and the deflection parameter *K* is proportional to the product of the magnetic period and peak on-axis field  $B_u$ ,

$$K = 0.93 B_u [\text{T}] \lambda_u [\text{cm}].$$

From this equation it is easy to show that, in order to achieve X-ray wavelengths of 1 Å with a 2.8 GeV electron energy ring, even using the third harmonic, requires magnetic periods of the order of 1 cm. The performance of such a magnet is enhanced by simultaneously reducing the gap between the magnet structures proportionally.

Countering the arguments for reduced gap are concerns about the impact of small gaps on the stored electron beam, in particular the lifetime of the electron beam. A prototype small-gap undulator (PSGU) was designed and installed at X13 in 1993 to explore the small-aperture limit for the electron beam in the NSLS X-ray ring (Stefan & Krinsky, 1996; Stefan *et al.*, 1995, 1996). In studies, the PSGU was operated with gaps as small as 3 mm without effect on the X-ray ring lifetime, even with a stored beam of 300 mA at 2.584 GeV. The next stage of small-gap undulator development, the in-vacuum undulator (IVUN), was constructed with an 11 mm period (62 poles) and contained 31 periods. The IVUN was installed at the center of the X13 R&D straight section of the NSLS X-ray storage ring in May 1997, where it replaced the PSGU device

(Rakowsky *et al.*, 2001; Stefan *et al.*, 1998; Tanabe *et al.*, 1998). During study periods, the IVUN operated with magnet gaps between 10 mm and 3.2 mm, with the NSLS storage ring operating at 2.8 GeV. The beam lifetime was essentially constant from 10 mm to 4.5 mm. Even at the 3.2 mm gap, the lifetime has only decreased from 14 h to about 12.7 h.

During 2001, the IVUN device was replaced by an in-vacuum MGU that provides better tunability than IVUN (Ablett *et al.*, 2004). The MGU has a magnetic period of 12.5 mm and is comprised of 54 poles of permanent NdFeB magnets with vanadium permendur poles. It was installed at the center of the X13 straight section where the vertical  $\beta$ -function is minimized. Operating down to a gap of 3.3 mm, it delivers a magnetic field of 0.92 T with a deflection parameter  $K$  of about 1.07. High-brightness X-ray photon beams are delivered in the first, second and third harmonics, tunable within the energy ranges 3.7–5.5 keV, 7–10 keV and 11.2–16 keV, respectively.

The MGU device at X29 is similar to the one currently installed at X13. The X29 MGU has a 12.5 mm period and effectively 27 periods (54 poles). This device has a deflection parameter  $K$  of 1.17, a fundamental energy of 3.5 keV, and a tuning range of about 50% (3.5–5.5 keV). The peak field ( $B_u$ ) at 3.3 mm gap, computed by the three-dimensional magneto-statics code *Radia* (free and available for download from the ESRF web site [http://www.esrf.fr/Accelerators/Groups/InsertionDevices/Software/Radia/Radia\\_download](http://www.esrf.fr/Accelerators/Groups/InsertionDevices/Software/Radia/Radia_download)), is 1.0 T. The corresponding tuning range of the third harmonic is 11–15 keV. Owing to the emittance of the X-ray ring not being extremely small, there is also a significant second harmonic on-axis, which broadly covers 5–10 keV.

Brilliance differences determine the ultimate throughput of any optical system. A direct comparison of theoretical brilliance between the former X25 wiggler and the X29 MGU at a fixed gap (3.3 mm) is shown in Fig. 1. The theoretical brilliance of X29 is about sixfold greater for the third harmonic (11.3 keV). The brilliance of an APS undulator-A in

the (widely tunable) first harmonic ( $\sim 7$  keV) is  $\sim 3 \times 10^{19}$  photons  $s^{-1}$  (0.1% bandwidth) $^{-1}$  mrad $^{-2}$  mm $^{-2}$  (100 mA) $^{-1}$  (Dejus *et al.*, 2002), which accurately reflects the operating ring current of 100 mA at APS. The curve of Fig. 1 assumes 1 A at the NSLS, while the actual maximum current is  $\sim 300$  mA. Thus, the theoretical brilliance of the X29 undulator is  $3 \times 10^{17}$  per 300 mA, or  $\sim 100$  times less brilliant (in theory) than the APS station. It should be noted that the actual experience of crystallographers at the APS is that the beam is mostly not used in fully focused mode and is often attenuated. For example, at SBC-CAT attenuation factors of five- to ten-fold are often used. This implies that this device may be only 10–20 times less brilliant than APS undulators for most experiments.

Owing to the small dimensions, tight dimensional tolerances and precise pole positioning are required. Poles sit on the ground surface of an aluminium base plate and are anchored by screws threaded into vented holes in the pole bottoms. Longitudinal indexing and pole alignment is accomplished by a tongue-and-groove interface between the pole ends and the aluminium side rails. Magnets fit into channels cut into the base plate and into notches in the side rails and are held in pairs by clamps bearing on the magnets' chamfered corners. Building on the success of the IVUN design, the MGU uses the same vacuum chamber and support structure, except for symmetric transitions, to accommodate the RF straight symmetry, and heavier through-vacuum members of the gap-adjusting mechanism to handle the higher magnetic forces in the MGU.

Previously there was no insertion device in X29, so the existing dipole exit chamber had been constructed with 2.5° and 10° ports. Consequently an all new dipole chamber design was required. The new chamber, which was installed in December 2002, has ports for 0°, 3.5° and 10° beamlines. The 10° port serves the existing NSLS short diagnostic beamline, the 3.5° port is currently capped with a water-cooled OFHC (oxygen-free high-conductivity) copper absorber, awaiting possible future service, and the 0° port serves the new X29 beamline. The dipole chamber is a completely new design and includes a NEG pump, a distributed ion pump, fixed cooling-water channels around the exit slots, and removable OFHC copper crotch absorbers. In addition, an all new active interlock system was designed, installed and tested to insure precise control of the electron-beam orbit excursion limits (from nominal) through the MGU.

### 3. X29 front-end and optical system

For optimal performance, the magnification of the optics should be chosen so that the beam size at the sample matches the sample size, and the spot size at the detector matches the spatial resolution of the detector. When focusing on the sample, too little demagnification results in only a fraction of the beam passing the slits, whereas too much demagnification leads to divergence which makes spots on the detector too large.

Optics optimization requires being able to move the horizontal focus freely between collimator and detector over

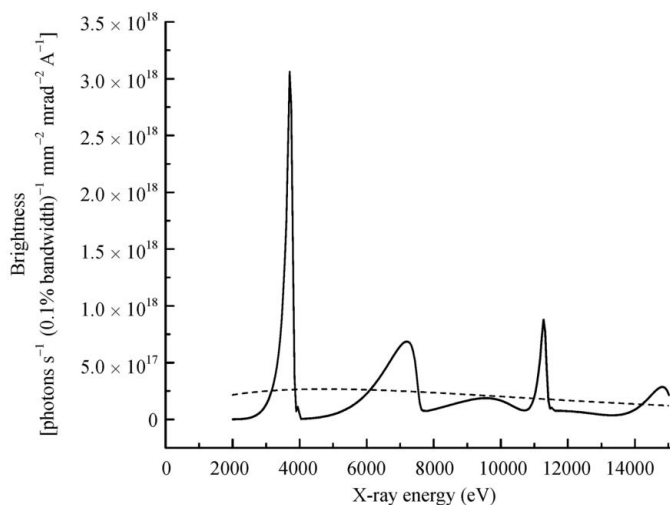


**Figure 1**  
Theoretical brightness curves from X25 (dashed line) compared with the X29 MGU operated at a fixed gap of 3.3 mm (solid line). Ring energy is 2.8 GeV.

the whole range of detector distances in order to maximize the flux through the slits without adversely affecting the spot size on the detector. Horizontal focusing by sagittally bending of the second crystal of the monochromator provides free choice of focal length over a wide range (Habenschuss *et al.*, 1988).

A schematic drawing of the X29 front-end and optics is shown in Fig. 2. When the beam is focused on the sample, its horizontal demagnification is 4.1:1. This will generate a horizontal beam width of about 0.15 mm FWHM and a horizontal convergence angle of 1.9 mrad. This would be well matched for 0.10–0.15 mm defining slits. For a detector distance of 200 mm, the spot size would be about 0.45 mm. The spot broadening could be reduced by focusing a bit closer to the detector, with a concomitant loss of transmission through the slits.

The space for the X29 beamline port was severely restricted owing to the nearness of the booster-ring shield wall. To maximize usable beamline space, the X29 ‘sawtooth’ shield wall and the X29 front-end were completely re-designed. This entailed the design of all new front-end and optical components, including a water-cooled fixed primary aperture mask, Be window, water-cooled adjustable primary aperture, cryogenically cooled double-crystal monochromator with sagittally focusing second crystal, vertical focusing mirror, Bremsstrahlung collimator, white/monochromatic beam shutter, combined vacuum tank for the monochromator and mirror, safety interlocks, and structural supports for minimal size and maximum structural stability.

The front-end components were designed to withstand thermal exposure twice as great as calculated for worst-case MGU output. Since the option of locating all or a part of the primary aperture and optics inside the shield wall is impractical in terms of access, the stacked concrete sawtooth section of the shield wall (ratchet wall) was relocated 1.86 m closer to

the source at 10.6 m, now enclosing the tailpipe of the first Bremsstrahlung collimator. To accomplish this, the 27 inch-thick wall constructed of standard concrete was replaced by a heavy concrete block construction 16 inches thick. A new pre-cast concrete access door with air lifters and path guides was designed, fabricated and installed as well.

The X29 front-end inside the ratchet wall includes a modified water-cooled aperture at 8.85 m. The aperture has been reduced to a size slightly larger than the size of the usable beam, allowing the size of the tailpipe and the opening of the Bremsstrahlung collimator to be reduced. This helped to narrow drastically the size and the angle of the extreme rays of the Bremsstrahlung cone.

The first beamline component outside the ratchet wall is a metal valve interlocked through the beamline interlock system that will close the safety shutter if the valve is closed during operations (Fig. 2). The beamline components downstream of the metal valve up to the monochromator tank include a water-cooled mask, a Be window and a water-cooled adjustable primary aperture. The water-cooled mask absorbs the bulk of the beam power to protect the downstream Be window from thermal overloading. With 453 W of the total beam power of 588 W absorbed at closed gap and 350 mA beam current, the power passing through the mask is 135 W. The Be window consists of a Be foil of 0.5 mm thickness brazed to a copper frame attached to the end of the water-cooled aperture mask (Rosenbaum *et al.*, 2006). The total power absorbed in the Be window is 35 W at closed gap. Immediately downstream of the Be window is a water-cooled adjustable primary aperture. This device allows the horizontal and vertical size of the beam to be defined; in addition it provides a tool for beam diagnostics. It helps to reduce the power load on the monochromator and to reduce thermal drift. It has the ability to close to approximately a 30 µm gap and allows scanning of this slit across the beam.

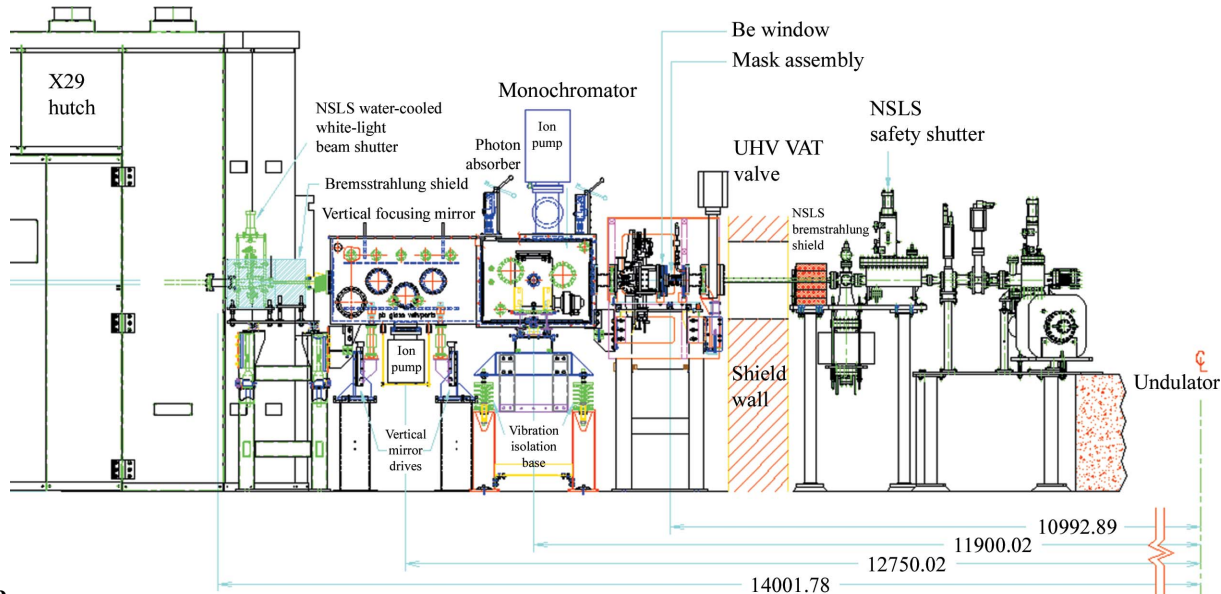


**Figure 2**  
Schematic drawing of the X29 front-end and optical system.

The optical system is an adaptation of the system installed at 22-ID of SER-CAT, which is based on the design of 19-ID of SBC-CAT at the APS (Rosenbaum *et al.*, 2006). Owing to the extreme space limitation at X29, the monochromator and the downstream mirror are compressed into a combined vacuum tank (Fig. 2). X29 is equipped with a cryogenically cooled sagittally focusing monochromator, with the first crystal located at 11.9 m from the source. The double-crystal monochromator is the upstream element that selects the energy, maintains the beam at a constant exit height, and focuses the beam in the horizontal direction.

The X29 monochromator has two unique features. The first is that the first crystal is directly cooled with helium gas (Berman *et al.*, 2002) by a modified Cryomech cryogenic cooling system at 100 K. Two Cryomech compressors in combination with a heat exchanger system supply the cold He gas directly to the back of the finned first crystal. The crystal is encased in a helical seal wrapped with indium foil. The compressor system is designed to run at 80 p.s.i., too high for the crystal seal. A regulator was incorporated into the system to lower the pressure. Since the cooling capacity is proportional to the pressure, an over-sized system was required to provide adequate cooling power to maintain the temperature of the first crystal around 100 K.

The second unique feature of the X29 monochromator is that the second crystal is a thin Si (111) semiconductor wafer bonded to aluminium finger wings with a dimension of 35 mm × 75 mm × 350 µm (the longest dimension in the direction of the beam). The crystal is very thin (350 µm) allowing it to be elastically bent by a four-pin bending fixture into a cylinder (axis in the plane of diffraction). Ribless thin-crystal technology has been around for many years, but this is usually done by cutting the crystal from a large ingot and is very expensive. The thickness of the crystal is chosen to be as thick as possible so that for the minimum bending radius, given by the minimum focal length and the minimum Bragg angle, the strain in the Si wafer is safely below the breaking limit. The springs of the bender that convert the motion of the focusing motor into a bending moment on the Si wafer are chosen so that for the thickness of the crystal in use the minimum bending radius is achieved at about 3/4 of the range of the focusing motion. These factors, including the crystal thickness, bender capabilities, pin friction, spring force and focusing reproducibility, were the determining parameters of the present focusing crystal at X29. This design has been proven to be of equal performance to the monolithic design used at other synchrotron beamlines.

A water-cooled copper block (photon absorber) was installed inside the monochromator to absorb the direct photon beam downstream of the monochromator. A vertical focusing mirror is used for harmonic rejection, and can provide vertical focusing. It is installed downstream of the monochromator in a combined vacuum tank at 12.75 m (Fig. 2). It collects all of the vertical divergence from the source, and provides vertical focusing when elastically bent to a cylinder (axis orthogonal to the optical plane). Independent benders at each end of the mirror allow an elliptical bending

correction for elimination of spherical aberrations. The X29 mirror has a 'striped' configuration where 1/3 is (uncoated) ULE substrate (ultra-low-expansion titanium silicate), 1/3 is palladium and 1/3 is platinum-coated. A lateral translation moves the appropriate coating into the beam when the photon energy is changed so that, without changing the mirror angle, the fundamental is reflected but the third harmonic passing the monochromator is rejected. The vertical demagnification at X29 is about 5.8:1.

Immediately downstream of the monochromator/mirror tank is a Bremsstrahlung collimator followed by a water-cooled NSLS white-light shutter, the last beamline component before entering the X29 hutch (Fig. 2). Both units are mounted on a vertical-positioning table which can also be tilted to the angle of the mirror-deflected beam. The shutter is the standard NSLS design used as safety shutters on several white-light beamlines around the ring including X13, which is also an undulator beamline. A Be exit window is located immediately inside the experimental end-station enclosure.

#### 4. X29 experimental station

The experimental station is equipped with an ADSC (Area Detector Systems Corporation) Q315 detector with 100 µm resolution and near 2 s readout time (Fig. 3). The Q315 detector is coupled with a Crystal Logic large detector goniostat for detector positioning and crystal rotation. The detector operates in the distance range of 90–700 mm from the sample. The goniostat includes a motorized mini- $\kappa$  drive to rotate the crystal mount to 50° from the horizontal for the mounting of frozen crystals. This rides on a tripod-based motorized X–Y–Z orienter (this provides a click-to-center option for easy operation). In addition, the mini- $\kappa$  drive allows one to change the axis around which the specimen crystal rotates. In combination with the large CCD detector, this facilitates data collection on crystals with large unit cells. The defining apertures are motorized and adjustable.

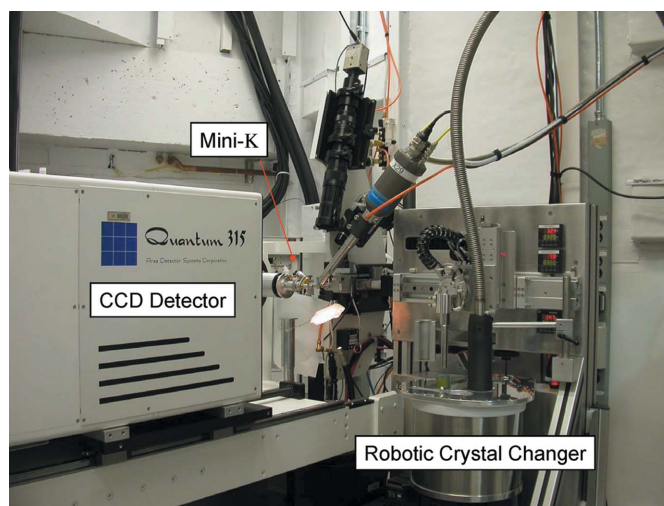


**Figure 3**  
The X29 experimental station.

An auto-mounter crystal changer is installed at X29 to facilitate fast automated data collection (Schneider *et al.*, 2006). The X29 auto-mounter offers a newly designed liquid-nitrogen dewar which is thermally improved, mechanically more accurate and features a puck access door on the dewar lid. The X29 auto-mounter accommodates several designs of crystal mounting caps. Details of how to plan a data-collection trial using the auto-mounter are posted on the X29 website ([http://www.px.nsls.bnl.gov/x29/x29\\_info.html](http://www.px.nsls.bnl.gov/x29/x29_info.html)).

### 5. X29 control system

The success of a beamline depends on its stability and ease of use. At X29 the beamline staff have been striving to make the beamline more automatic for high-speed operation and easy to use by a wide range of scientists. All moveable components of the X29 X-ray optics are adjusted by 12 V servo motors. These servo motors are controlled by a custom design motor control interface which utilizes a CAMAC-based E500 stepper controller and a computer with Windows XP operating system with *Labview* software (National Instruments). This system has proven to be extremely reliable and accurate, and is employed at all five beamlines built by the Case Western Reserve University Center for Synchrotron Biosciences. The motor control interface is capable of operating with any stepper-motor controller such as Compumotor and VME, and is controllable by any computer operating system including Linux and Macintosh.

During X29 commissioning (May–December 2004), users were instructed to make simple changes through the basic beamline control system, such as changing the wavelength, and the focus of the second crystals. In addition, excitation scans at particular heavy-atom edges were made with the beamline control system. Gradually, these functions were merged into the X29 experimental station control system (see below, and Skinner *et al.*, 2006). Currently, the beamline control system is only operated by the beamline staff for tasks including checking the beamline motor positions and for special data-collection requirements such as shifting the beam focus position from the defining aperture towards the detector for crystals with long cell dimension.

The control system for the end-station at X29 is called CBASS (Skinner *et al.*, 2006). It controls the in-hutch motors and allows one to perform beam optimization and to set up data-collection runs. It links to the NSLS undulator gap system through EPICS (Experimental Physics and Industrial Control System) (<http://www.aps.anl.gov/epics/>) and communicates to the beamline optics control system (*Labview*) so that the energy change, beam focusing and gap shift occur simultaneously and transparently without direct intervention from the user.

CBASS is also connected to the Protein Crystallography Database (PXDB) (Skinner *et al.*, 2006) maintained by the Macromolecular Crystallography Research Resource (PXRR) group. Users can create an account, request beam time and fill out an end-of-run form in PXDB. PXDB also serves as a useful administrative tool for beamline staff to review data-

collection sweep reports from the users. In addition, PXDB is 'robot ready'. Information for crystals intended for the auto-mounter crystal changer can be entered by users in PXDB at home institutions and retrieved in CBASS during data collection.

### 6. X29 performance

The focused spot size at 11.271 keV (1.1 Å) was measured to be 180 µm × 120 µm FWHM (horizontal × vertical) for X29. The horizontal FWHM is consistent through an energy range of 7–15 keV. The vertical FWHM varies by twofold in the same energy range without optimization of the motor control configuration for the vertical focusing mirror. The beam is normally focused at the defining aperture which is approximately 5.5 cm upstream of the sample position. Most X29 users are satisfied with this arrangement. The horizontal focus of the beam can be easily shifted by adjusting the focusing motor of the second crystal in the X29 beamline control system. When collecting data with a large unit cell, the focus of the beam is sometimes shifted downstream at the sample position or at the detector both to minimize the size of diffraction spots and to increase the separation of the spots.

X29 is optimized at 11.271 keV (1.1 Å), and approximately half of the data are collected at this wavelength. The defining aperture at X29 is a motorized square aperture set normally at 120 µm × 120 µm. The measured fluxes at the sample position at this energy and with the beam focused on the defining aperture at this setting is  $2.5 \times 10^{11}$  photons s<sup>-1</sup>. This flux is less than that with an open aperture since the focused beam spot is larger than the size of the defining aperture. At 1.1 Å the flux with an open defining aperture is approximately three times that measured with a 120 µm × 120 µm aperture.

X29 is used for protein crystallography, which requires a bright X-ray beam in the energy range 7–15 keV. The measured flux through the 120 µm × 120 µm square aperture, and through the open aperture, is shown in Fig. 4 for the energy range 7–15 keV. The point of this is to show that, even though the third harmonic of the X29 undulator produces the maximum intensity at 11.271 keV when the gap of the undulator is completely closed, the shoulder of the third harmonic is broad enough to cover the energy gap between the second and third harmonics (10–11 keV) to deliver approximately half of the maximum flux in this range, providing serviceable flux for MAD data collection. Osmium, a heavy-atom element commonly used for protein crystallography phasing, has an edge of 10.876 keV. The average exposure time is 3 s per frame at X29. A three-wavelength MAD data set is usually completed in less than 60 min.

### 7. X29 operation

X29 supports structural genomics projects and a mail-in program whereby researchers mail cryo-preserved specimens by fast courier to the NSLS and PXRR scientific staff oversee data collection and often structure solving (Robinson *et al.*, 2006). The NIH-funded New York Structural Genomics

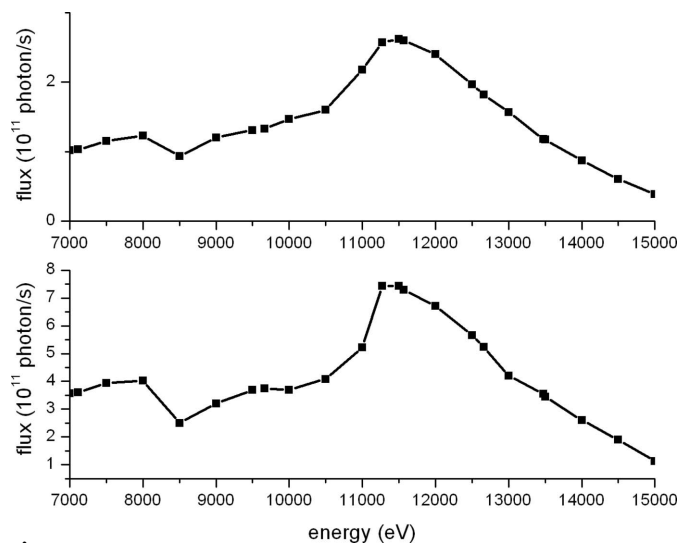


**Figure 4**  
X-ray beam flux measured at X29. The measurement is normalized to 300 mA ring current. The X-ray beam is focused on a defining aperture about 5.5 cm upstream of the crystal. Top panel: measured flux through a  $120\ \mu\text{m} \times 120\ \mu\text{m}$  square aperture. Bottom panel: flux through an open defining aperture.

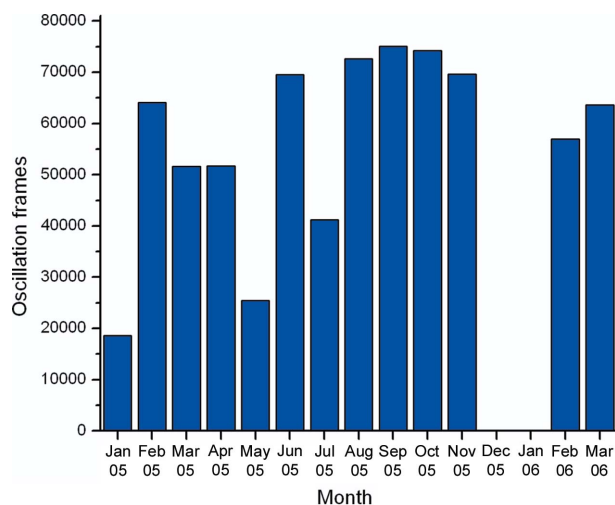


**Figure 5**  
Oscillation frames collected at X29 by month (from January 2005 to March 2006).

Research Consortium utilizes 30% of X29 beam time through the Case Center for Synchrotron Biosciences. PXRR of BNL Biology Department organizes the mail-in project and the Rapid Access beam-time request program. Part of the beam time during daytime on weekdays is used for beamline maintenance and development when necessary. These developmental tasks include tuning the beamline optics for flux improvement, and installation and testing of the robotic crystal changer. Other daytime slots on weekdays are scheduled for those users with quick projects which can be carried out in 2–8 h. If more beam time is needed to finish the project, beam-time requests through the Rapid Access program allow the users to come back in about two weeks time.

X29 is an extremely productive beamline with an average of two to three groups of users scheduled every day to perform

data collection. Near 400 users have been trained and have collected data at the beamline since June 2004. The oscillation frames collected at X29 by month is shown in Fig. 5. As of July 2006, 84 structures have been deposited in the Protein Data Bank credited to X29. The user-friendly operation and the convenient location of X29 attract a large number of productive structural biology groups from the Mid-Atlantic and New England regions of USA.

## 8. Future development

Built on the promise of the X29 device, X25 is undergoing an upgrade to replace the existing wiggler with a new MGU. The new X25 undulator is a variant of the X13 and X29 devices with a longer period and a wider gap, and will have higher brightness and continuous energy tunability from 2 to 20 keV. In addition, it incorporates provisions for cryogenic operation to be pursued in the future providing a broadly tunable energy range throughout the third to ninth harmonics providing an almost continuous bright X-ray beam (Rakowsky *et al.*, 2006).

NSLS is involved in a collaborative effort of all DOE (Department of Energy) synchrotron radiation facilities in development and use of advanced superconducting undulator devices, which provide a much brighter hard X-ray beam compared with traditional permanent-magnet undulator devices. This technology will have great impact on NSLS II which has recently been granted CD-0 status by the DOE; these undulator developments will be of benefit to synchrotron radiation facilities worldwide.

We are grateful for the National Institute for Biomedical Imaging and Bioengineering Biomedical Technology Resource program, grant P41-EB-01979 to Case Western Reserve University; NIGMS Protein Structural Initiative, grant P50-GM-62529 to the New York Structural Genomix Research Consortium at SGX Pharmaceuticals; NIGMS and NCCR grants N1-GM-9069-01 and Y1-RR-9004-01 to NSLS; and NIH National Center for Research Resources, grant P41-RR-012408 to the BNL Biology Department. Contribution to X29 by the National Synchrotron Light Source, Brookhaven National Laboratory, which is supported by the US Department of Energy, Office of Science, Office of Basic Energy Sciences, under Contract No. DE-AC02-98CH10886, is also acknowledged.

## References

- Ablett, J. M., Berman, L. E., Kao, C. C., Rakowsky, G. & Lynch, D. (2004). *J. Synchrotron Rad.* **11**, 129–131.
- Berman, L. E., Siddons, D. P., Montanez, P. A., Lenhard, A. & Yin, Z. (2002). *Rev. Sci. Instrum.* **73**, 1481–1484.
- Dejus, R. J., Vasserman, I. B., Sasaki, S. & Moog, E. R. (2002). APS Technical Bulletin ANL/APS/TB-45. APS, ANL, Argonne, IL, USA.
- Habenschuss, A., Ice, G. E., Sparks, C. J. & Neiser, R. (1988). *Nucl. Instrum. Methods*, **A266**, 215–219.
- MacDowell, A. A. *et al.* (2004). *J. Synchrotron Rad.* **11**, 447–455.
- Rakowsky, G. *et al.* (2006). Personal communication.

- Rakowsky, G., Lynch, D., Blum, E. B. & Krinsky, S. (2001). *Proceedings of the 1995 Particle Accelerator Conference*, Chicago, IL, USA, pp. 2453–2455. Piscataway, NJ: IEEE.
- Robinson, H., Soares, A. S., Becker, M., Sweet, R. & Héroux, A. (2006). *Acta Cryst. D* **62**, doi:10.1107/S0907444906026321.
- Rosenbaum, G. *et al.* (2006). *J. Synchrotron Rad.* **13**, 30–45.
- Schneider, D. *et al.* (2006). Personal communication.
- Skinner, J. M., Cowan, M., Buono, R., Nolan, W., Bosshard, H., Robinson, H. R., Héroux, A., Soares, A. S., Schneider, D. K. & Sweet, R. M. (2006). *Acta Cryst. D* **62**. In the press.
- Stefan, P. M. & Krinsky, S. (1996). *Rev. Sci. Instrum.* **67**, 3394. (Full text on CD-ROM only.)
- Stefan, P. M., Krinsky, S., Rakowsky, G. & Solomon, L. (1995). Report LBL PUB-754, pp. 161–173. Lawrence Berkeley National Laboratory, Berkeley, CA, USA.
- Stefan, P. M., Krinsky, S., Rakowsky, G. & Solomon, L. (1996). *Proceedings of the 1995 Particle Accelerator Conference*, Dallas, TX, USA, pp. 2435–2437. Piscataway, NJ: IEEE.
- Stefan, P. M., Krinsky, S., Rakowsky, G., Solomon, L., Lynch, D., Tanabe, T. & Kitamura, H. (1998). *Nucl. Instrum. Methods, A* **412**, 161.
- Tanabe, T., Marcechal, X. M., Tanaka, T., Kitamura, H., Stefan, P., Krinsky, S., Rakowsky, G. & Solomon, L. (1998). *Rev. Sci. Instrum.* **69**, 18–24.